Cyclones and associated weather patterns over the northern North Atlantic region based on ECMWF reanalyses

Nikolai Nawri
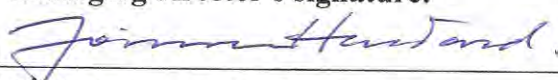
Veðurstofa
Íslands

Cyclones and associated weather patterns over the northern North Atlantic region based on ECMWF reanalyses

Nikolai Nawri, Icelandic Met Office

Veðurstofa Íslands

Keypage

Report no.: VÍ 2015-005	Date.: September 2015	ISSN: 1670-8261	Public ☒ Restricted ☐ Provision:
Report title / including subtitle Cyclones and associated weather patterns over the northern North Atlantic region based on ECMWF reanalyses			**No. of copies:** 4 **Pages:** 35
			Managing director: Jórunn Harðardóttir
Author(s): Nikolai Nawri			**Project manager:** Halldór Björnsson
			Project number: 5818-0-0001
Project phase:			**Case number:** 2015-239

Report contracted for:

Prepared in cooperation with:

Summary:

The short-term and seasonal weather conditions over Iceland and across Northwest Europe strongly depend on the location and intensity of dominant low-pressure centres over the northern North Atlantic and Nordic Seas. In winter, the region with the highest cyclone density is found between Iceland and the southern tip of Greenland. Other regions with a high wintertime cyclone occurrence are located over the Norwegian and Barents seas, as well as southwest of Greenland and over Baffin Bay. Different preferred regions of surface cyclone development are activated by relatively small shifts in the mid- and upper-level tropospheric circulation, and surface weather conditions across the northern North Atlantic region are significantly affected by these shifts.

Keywords: ERA-40 and ERA-Interim Reanalyses Cyclones, Large-scale weather patterns Surface air temperature Surface wind speed, Precipitation Northern North Atlantic	**Managing director's signature:**
	Project manager's signature:
	Reviewed by: Trausti Jónsson, SG

Contents

List of Figures

1 Introduction

Extratropical low-pressure systems, persisting for at least a few days, have long been recognised as one of the main drivers of surface weather conditions, particularly for strong low-level winds and intense precipitation (Bjerknes, 1919; Bjerknes & Solberg, 1922). Since the 1990s, with increasing availability of global gridded datasets from reanalyses and climate simulations, a large number of studies have been dedicated to developing methodologies for the automated identification and tracking of extratropical storm systems (for a review, see Ulbrich, Leckebusch, & Pinto, 2009). These numerical procedures either emulate methodologies of manual analyses based on the printed charts of previous decades, or introduce more dynamical criteria for cyclone identification. In the traditional method, cyclones are identified as local minima of mean sea level pressure (MSLP), whereas in the dynamical method, the focus is on local maxima of relative vertical vorticity.

The continued use of two well-established methods for cyclone identification is due to the strengths and weaknesses inherent in both. Relative vorticity is better suited than MSLP to detect small-scale, fast-moving systems, such as polar lows, and is generally able to detect cyclonic storm systems at an earlier stage in their development. Also, MSLP is a poor indicator of cyclonic activity in tropical regions, where the geostrophic wind relationship breaks down (e.g., Anderson, Hodges, & Hoskins, 2003; Hodges, 1994; Hodges, Hoskins, Boyle, & Thorncroft, 2003, 2004; Hoskins & Hodges, 2002; Murray & Simmonds, 1991). With limited spatial resolution of gridded pressure data, there is the possibility that small or weak cyclones are masked by the trough of a planetary wave, or are only recognised as small perturbations of the MSLP field, unless the large-scale variability is filtered out. In those cases, the dynamical approach based on relative vorticity may also be more appropriate. However, for the same reasons, the use of relative vorticity can lead to serious over-detection. Local vorticity maxima may be due to the curvature of streamlines, such as along a trough axis, without the presence of any closed circulation. They may also be generated by speed shear between essentially straight streamlines, especially in connection with changes in surface roughness, such as for horizontal flow along steep coastal terrain (under stable conditions). This ambiguity between positive vertical vorticity maxima and cyclonic circulation is increased with the introduction of higher-resolution datasets, which may require spatial smoothing, to eliminate spurious vorticity extrema (Blender, Fraedrich, & Lunkeit, 1997; Hanson, Palutikof, & Davies, 2004; Sickmöller, Blender, & Fraedrich, 2000). As for high-pass filtering of the MSLP field, for the purpose of identifying weak low-pressure centres, this necessitates the subjective specification of several parameter values, which may affect the outcome of cyclone detection. To the extent that the large-scale flow is in geostrophic balance, relative vertical vorticity is proportional to the Laplacian of geopotential height. Therefore, vorticity can be derived either from first order derivatives (finite differentials) of the velocity field, or from second order derivatives of the geopotential height field. However, regardless of how vorticity is determined, it always requires the calculation of horizontal gradients, and is therefore sensitive to variable grid-point spacing (Sinclair, 1997). A hybrid approach was proposed by König, Sausen, and Sielmann (1993), where at their initial stages, cyclones are identified as relative maxima of vorticity at 850 hPa, but are considered for climatological analyses only if their centre depression on the 1000 hPa geopotential height field reaches at least 20 m relative to the 24 surrounding grid points over the course of their lifetime.

This study is concerned with well-developed, persistent, mid- to high-latitude large-scale weather systems, rather than their early detection and tracking. Therefore, cyclones will be determined here following the traditional method based on local MSLP minima, which are a better indicator of the large-scale circulatory flow structure than the local maxima of a more noisy and kinematically ambiguous relative vorticity field.

All winter (DJF) and summer (JJA) seasons during the 32-year period of 1979 – 2010 are included in the analysis.

The geographical focus is on the northern North Atlantic and the Nordic Seas. With the southern boundary at 47°N, the study domain covers Newfoundland, but excludes various marginal and inland seas with significant independent storm activity, such as the Mediterranean and Adriatic Seas, as well as the Black and Caspian Seas. The northern boundary at 80°N takes the domain up to Fram Strait, including Svalbard, but excluding Franz Josef Land. The western boundary at 71°W excludes Hudson Bay and Foxe Basin, both associated with their own storm climate. Baffin Bay is included in its entirety, since storm activity in that region is closely linked to that over the western North Atlantic (Dacre & Gray, 2009). The eastern boundary at 55°E is chosen to completely include the Barents Sea. This results in an area of 21,625,566 km^2, of which 60% are ocean.

This report is organised as follows. After describing the relevant data sources in Section 2, temporal correlations between MSLP and other atmospheric surface variables are discussed in Section 3. Section 4 introduces the methodology for the identification of cyclone centres. The spatial distribution of identified cyclone centres is discussed in Section 5. This distribution suggests a division of the study domain into three sectors, where the presence of cyclones in different sectors can be seen as being indicative of different modes of the MSLP field. The average mid- and upper-level tropospheric circulation involved in forming cyclones in the different sectors is discussed in Section 6, while the impacts on surface weather conditions, associated with different MSLP modes, are discussed in Section 7.

2 Data

The basis for this study are ERA-40 and ERA-Interim gridded reanalyses produced by the European Centre for Medium-Range Weather Forecasts (ECMWF) (Berrisford et al., 2009; Simmons, Uppala, Dee, & Kobayashi, 2006; Uppala et al., 2005). All reanalysis fields are available at a uniform 1-degree resolution in latitude and longitude. Over Iceland, this amounts to a physical grid-spacing of around 45 km in longitude, and 111 km in latitude. All variables, with the exception of precipitation, are provided as 6-hourly analysis fields valid at 00, 06, 12, and 18 UTC (which is local time in Iceland throughout the year). Six-hourly precipitation amounts at the four daily analysis times are derived by finite differentiation of grid-point time-series of total accumulation from the start time of each successive forecast run. To reduce spin-up effects, the first 12 forecast hours are ignored. Six-hourly precipitation on day D_0 is then calculated by differentiating the forecast run starting at 12 UTC on day $D_0 - 1$. Units of 6-hourly precipitation are kilograms per square metre. This is approximately equivalent to millimetres of liquid water.

Since, in this study, the focus is on large-scale storm systems, persisting for at least one day, variability on shorter time-scales (mainly the diurnal cycle and atmospheric tides) is eliminated by calculating averages from the four 6-hourly reanalysis fields of each day (6-hourly precip-
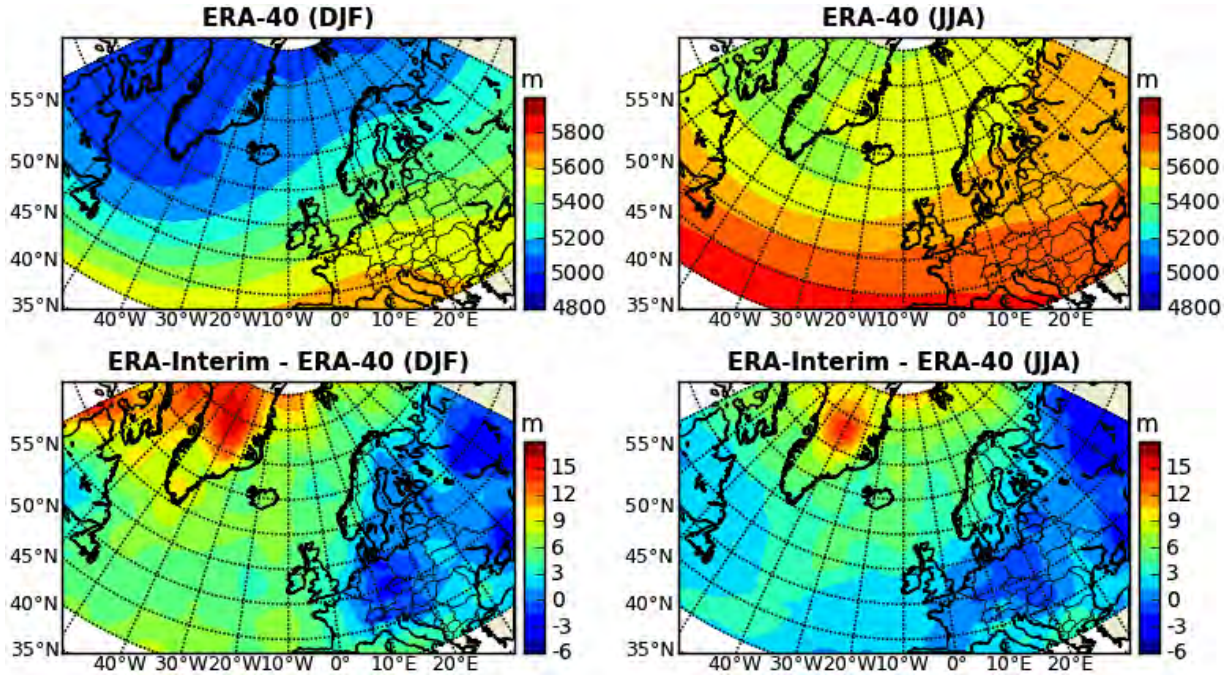
Figure 1. Top: Average fields of 500 hPa geopotential height in winter (DJF 1989-90) and summer (JJA 1990), based on the ERA-40 reanalysis. Bottom: Differences in 500 hPa geopotential height between the ERA-Interim and ERA-40 reanalyses.

itation amounts are added). Additionally, daily fields representative of longer-term conditions are calculated by applying centred running means over periods of 5 and 31 days to the daily time-series at each grid point.

The period covered by this analysis begins in 1979, with the use of satellite data in ECMWF reanalyses, and extends until and including 2010. With ERA-40 covering the 1958 – 2001 period, and ERA-Interim starting on 1 January 1989 leading up to the present, at some point within the study period, a transition needs to occur between the two reanalyses. However, as shown in Nawri (2013), significant differences exist for some variables between ERA-40 and ERA-Interim over Iceland. On a larger scale, comparisons between the two reanalyses are made here for seasonal mean fields during the winter (DJF) of 1989-90, and the summer (JJA) of 1990.

For 500 hPa geopotential height, the difference between the two datasets is shown in Figure 1. At mid-levels of the troposphere, there is a weakening of the northwest to southeast oriented pressure gradient across the study domain in ERA-Interim, relative to ERA-40, with the largest increase in geopotential height over Greenland, and the largest decrease over Continental Europe. At lower levels, possibly due to the constraints from surface measurements, differences in geopotential height are smaller (not shown).

MSLP in ERA-Interim, relative to ERA-40, is increased over Greenland by up to 3 hPa in winter, and up to 5 hPa in summer, with small and unsystematic differences elsewhere (not shown).

As shown in Figure 2, surface (10-m) wind speed in ERA-Interim is generally higher than in ERA-40. In coastal regions, over Iceland, and across southern Greenland, differences are up to 3 m s^{-1} in winter. Differences over the ocean are relatively small. Over land, differences are not
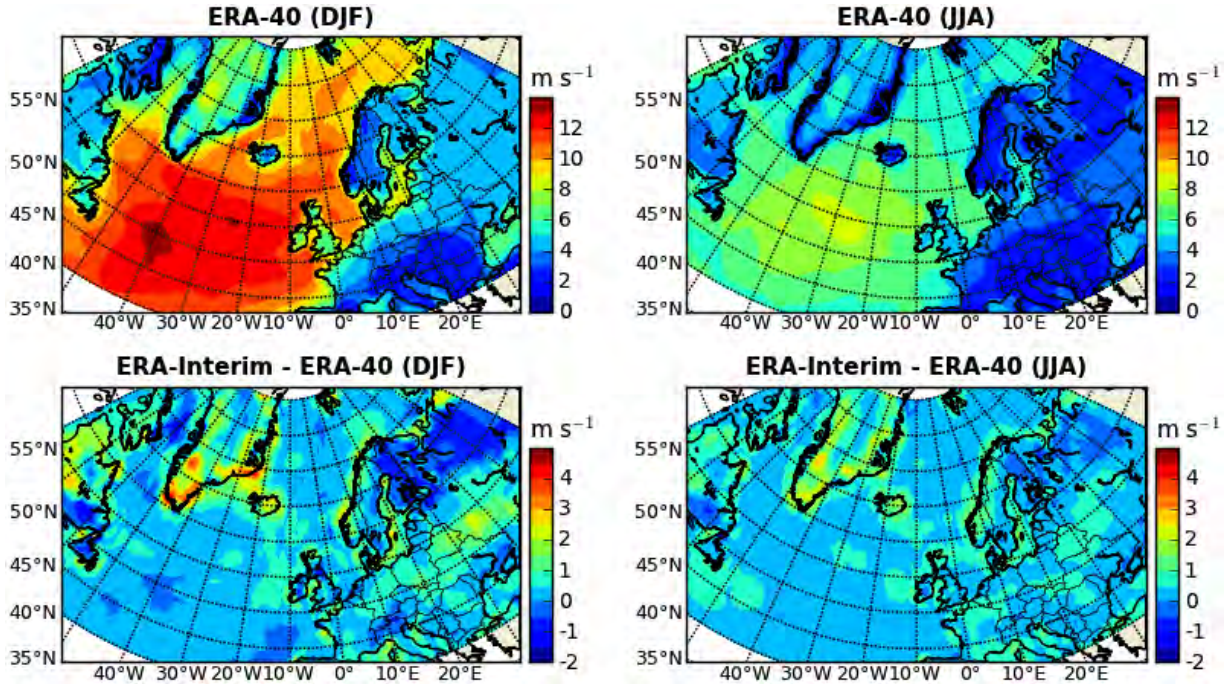
Figure 2. Top: Average fields of surface wind speed in winter (DJF) and summer (JJA), based on the ERA-40 reanalysis. Bottom: Differences in surface wind speed between the ERA-Interim and ERA-40 reanalyses.

in a simple manner related to terrain elevation, with negative values over the Alps, but positive and negative values across the East European Plain.

Surface (2-m) air temperature differences between the two reanalyses exist primarily over Greenland, where the amplitude of the seasonal cycle in ERA-Interim is reduced, with up to 5 K higher temperatures than ERA-40 in winter, and up to 5 K lower temperatures in summer (not shown). Elsewhere, differences are small and unsystematic.

As described by Simmons et al. (2006) and Berrisford et al. (2009), compared with ERA-40, several improvements in the ECMWF operational system were implemented for the ERA-Interim reanalysis project, leading to systematically improved forecast performance, especially with regard to the hydrological cycle. The most far-reaching changes include the introduction of a higher spatial resolution of the numerical weather prediction model, and more extensive use of different sets of satellite data. In general, ERA-Interim can therefore be considered to be more reliable, and was used here from its beginning in 1989 until 2010. For the earlier part of the period, 1979 – 1988, covered by ERA-40, daily fields are corrected as described in Nawri (2013).

Seasonal mean fields of mean sea level pressure, 500 and 250 hPa geopotential height, precipitation, sea surface and surface air temperature, based on the homogenised ERA-40 / ERA-Interim data, are shown in Figure 3. As found in earlier studies (e.g., Serreze, Box, Barry, & Walsh, 1993; Serreze, Carse, Barry, & Rogers, 1997), the Icelandic Low is the dominant feature of the seasonal low-level circulation across the northern North Atlantic. It is situated southwest of Iceland, downstream of a well-developed mean upper-level trough during the winter, but weakens and spreads northeast during the summer. The highest wintertime precipitation occurs southwest
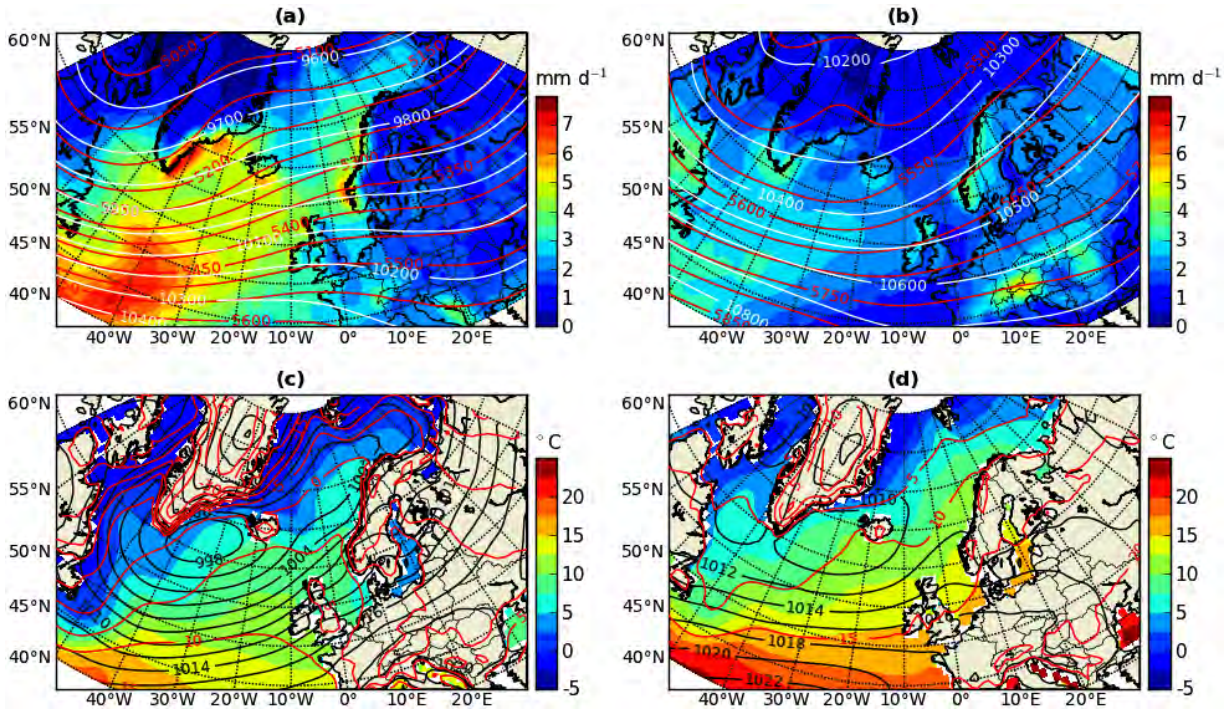
Figure 3. Seasonal mean fields in winter ((a) and (c)) and summer ((b) and (d)). (a) and (b): daily precipitation (coloured contours), 500 hPa geopotential height in metres (red contour lines), and 250 hPa geopotential height (white contour lines). (c) and (d): sea surface temperature (coloured contours), mean sea level pressure in hectopascals (black contour lines), and surface air temperature in degrees centigrade (red contour lines).

of the Icelandic Low, and ahead of the most intense baroclinic zone, representing the climatological cold front. High precipitation also occurs with forced ascent of onshore winds along the southwest coast of Norway, and the southeast coast of Greenland. In summer, the highest average precipitation occurs over elevated terrain (most notably the Alps) and in the vicinity of steep slopes.

3   Atmospheric variability connected to pressure changes

One of the oldest tools of instrument-guided weather forecasting is the analysis of local temporal tendencies in near-surface air pressure. This method is based on the fact that high pressure near the ground, relative to the local seasonal mean, is generally associated with low-level divergent flow, descending air throughout the troposphere, and consequently low cloudiness or clear skies, with little or no precipitation. Low pressure, on the other hand, is generally associated with low-level convergent flow, upward motion, clouds, and ultimately precipitation, if the atmosphere is sufficiently humid. Due to the low-level convergence, cyclones are more coherent systems than anticyclones, with generally steeper pressure gradients and therefore stronger low-level winds around the low-pressure centre.

However, this simple model does not take into account frontal or orographic effects. Therefore, in this section, it will be determined, to what extent temporal variability of air pressure, in a diverse geographical setting, is related to local temporal fluctuations of precipitation, and to
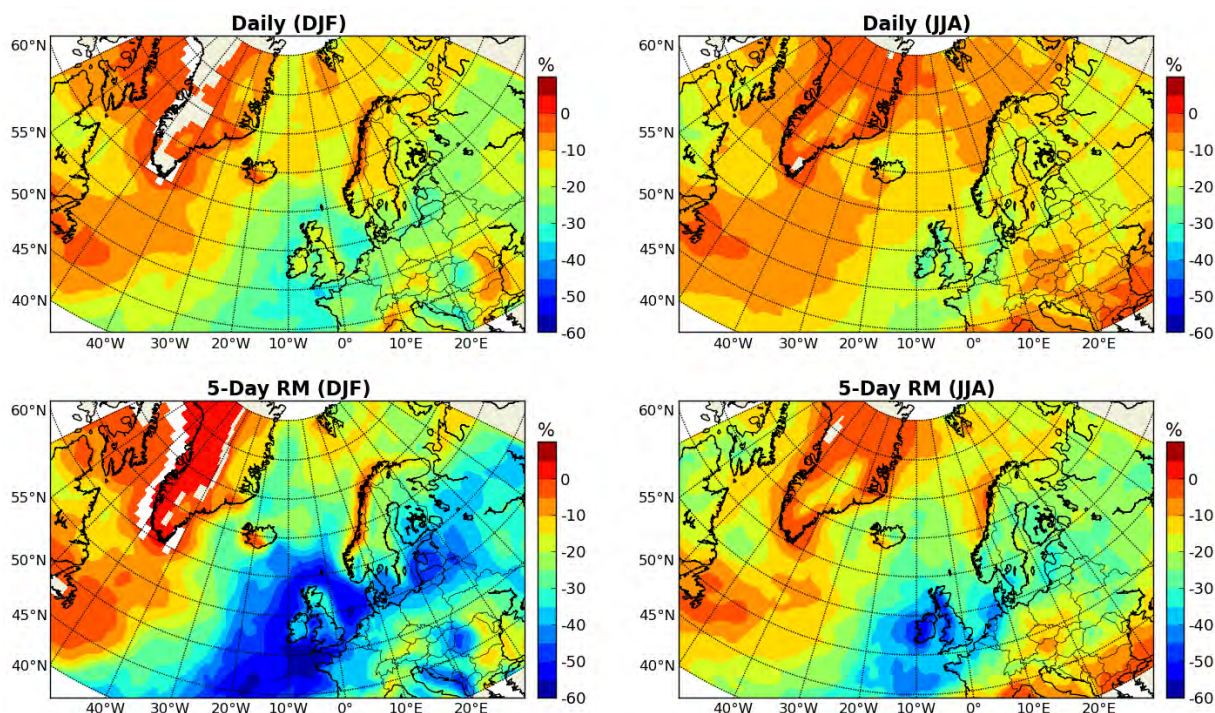
11

Figure 4. Coefficient of determination, with the sign of correlation, between mean sea level pressure and total daily precipitation in winter and summer, for grid-point time-series of daily averages (top row), and for 5-day running means of daily time-series (bottom row).

the zonal component of surface wind. In the following figures, the degree of temporal correlation between two variables is shown by means of the coefficient of determination (the square of the correlation coefficient), with the sign of the correlation coefficient, and multiplied by 100 (for units in percent). This gives the proportion of variance in the dependent variable, that is explained by a linear regression relationship with the forcing variable. Grid-point correlations are calculated separately for winter and summer months. This effectively removes the impact of the seasonal cycle.

The coefficient of determination between mean sea level pressure (MSLP) and total precipitation, is shown in Figure 4. Grid points at which correlation is not statistically significant at the 95% confidence level are omitted. Correlation between MSLP and precipitation is negative throughout most of the domain, as qualitatively expected based on the traditional forecast method. Quantitatively, however, variations in precipitation amount are not primarily related to local MSLP changes. The coefficient of determination is largest over the ocean ahead of the climatological cold front, extending southwest from the Icelandic Low (see again Figure 3). In that region, reduced MSLP is associated with an intensification of frontal dynamics, and increased forcing of precipitation. The coefficient of determination only exceeds 50% over the ocean south of the British Isles in winter, and for 5-day running means. Elsewhere, in other seasons, and on shorter time-scales, variance in precipitation is primarily due to fluctuations in atmospheric variables that are not directly linked to local MSLP changes.

Orographic effects on the interaction between MSLP and precipitation fluctuations are found over the western half of Greenland, where correlation between MSLP and precipitation in win-
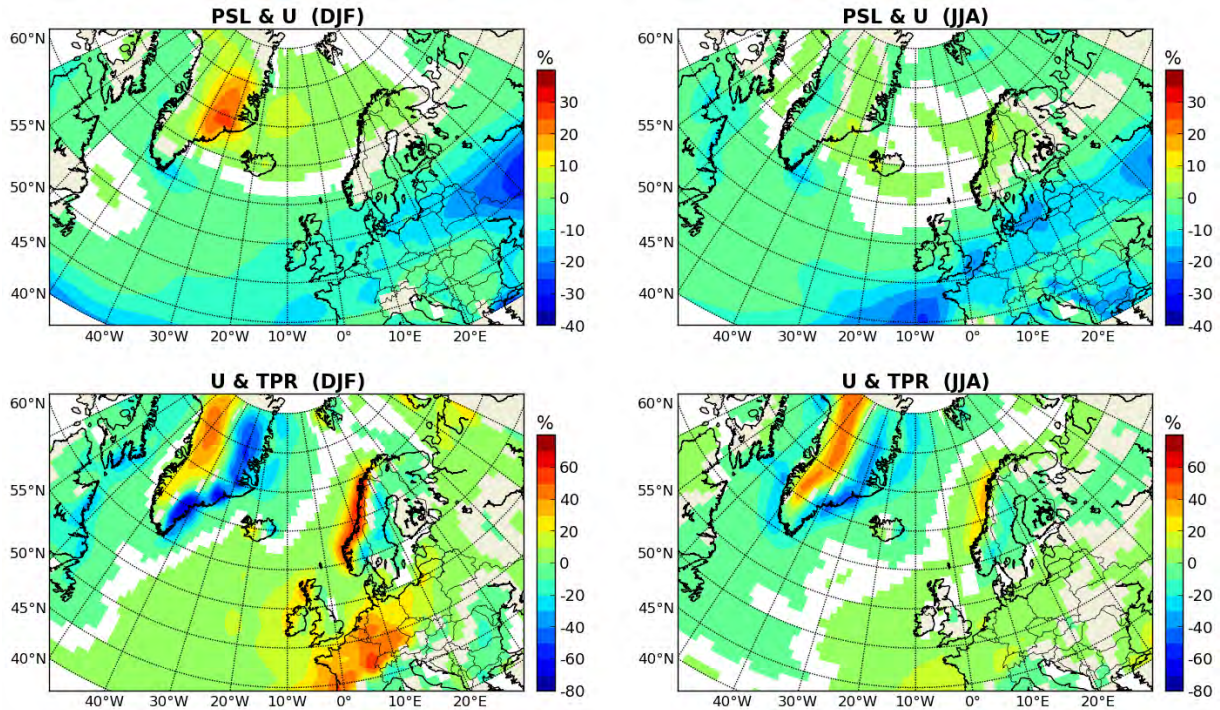
Figure 5. Coefficient of determination, with the sign of correlation, between mean sea level pressure and the zonal wind component (top row), as well as between the zonal wind component and total daily precipitation (bottom row) in winter and summer, for 5-day running means of daily grid-point time-series.

ter is slightly positive for 5-day running means. As shown in Figure 5, this is due to coupling via the zonal wind component. In winter, MSLP and the zonal wind component are positively correlated over Greenland, as well as over the ocean north of Iceland. Elsewhere in the domain, correlation is negative or negligible. There is an ambiguity in the temporal variability of individual velocity components. A positive change in the zonal wind component can either mean weakening of easterly winds, strengthening of westerly winds, or a shift from easterly to westerly winds. However, with prevailing easterly wintertime winds over Greenland, it can be assumed that positive changes in the zonal wind component are mostly due to a weakening of the large-scale circulation. Through the geostrophic wind relationship, this implies a weakening of the northward pressure gradient, and therefore a weakening of the Icelandic Low, relative to the semi-permanent high-pressure region over Greenland. The positive correlation over Greenland between MSLP and the zonal wind component suggests that, in that region, a weakened (strengthened) pressure gradient tends to be embedded in an overall pressure increase (decrease). The zonal wind component is positively correlated with precipitation over the western half of Greenland, and negatively over the eastern half. Given the prevailing easterly winds, the positive correlations are due to decreased precipitation with stronger downslope winds, while the negative correlations are due to increased precipitation with stronger upslope winds. In both cases, stronger winds are caused by a more intense Icelandic Low, embedded in an overall decrease in MSLP. Then, over the western half of Greenland, positive correlations between pressure and the zonal wind component combine with positive correlations between the zonal wind and precipitation.

13
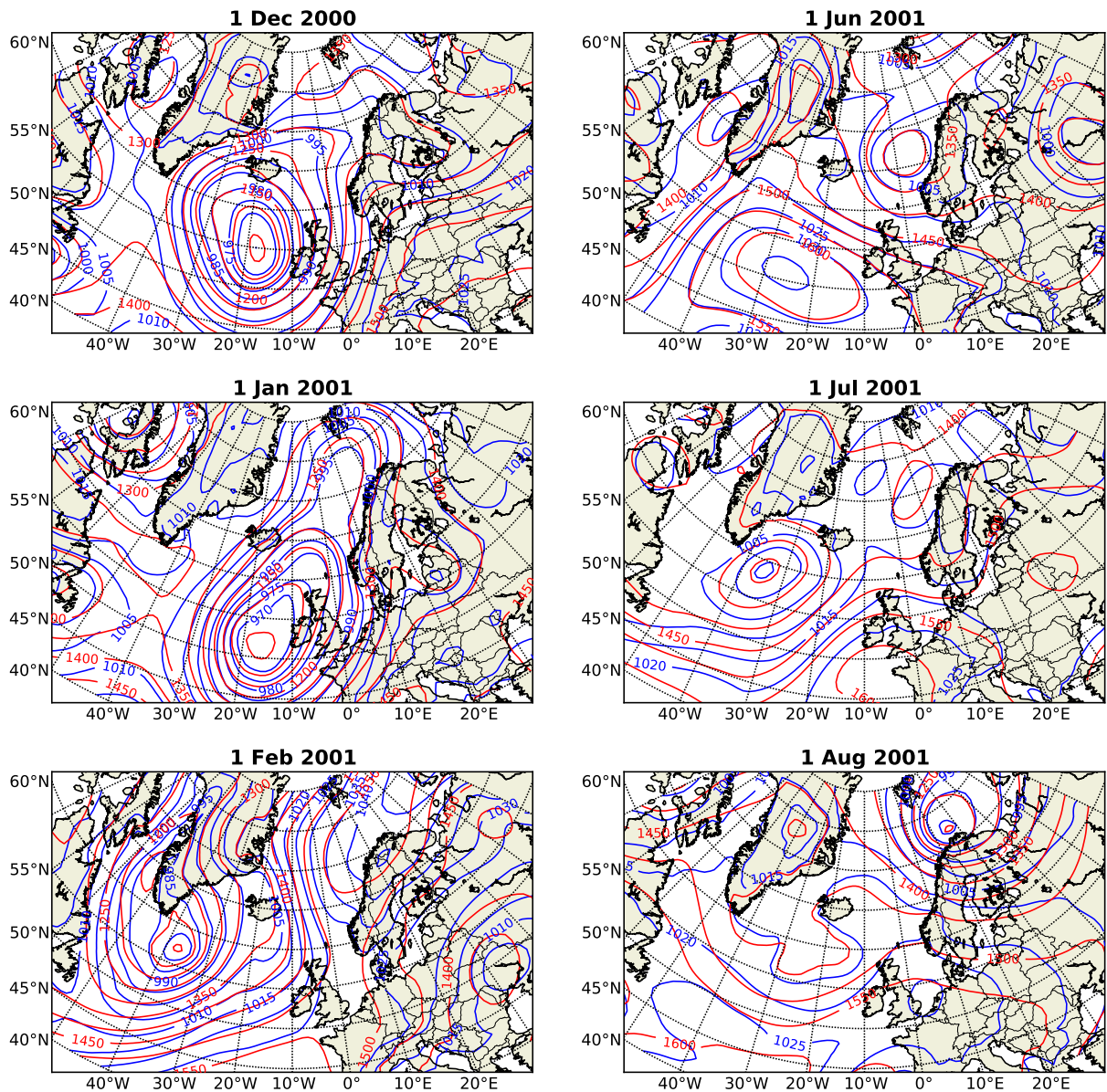
Figure 6. Daily reanalysis fields of mean sea level pressure in hectopascals (blue contours), and 850 hPa geopotential height in metres (red contours), in winter (left column) and summer (right column).

4 Identification of cyclone centres

Daily reanalysis fields of MSLP and 850 hPa geopotential height at the beginning of the 2000 – 01 winter months, and at the beginning of the 2001 summer months, are shown in Figure 6. In all these examples, there is at least one well-developed low-pressure centre present within the study domain. These weather systems have a recognisable cyclonic circulation, with closed isobars within up to about 1000 km from the pressure minimum.

These findings are compatible with more quantitative previous results. Using ERA-15 and NCEP-NCAR reanalyses, Hanson et al. (2004) identified cyclones as local minima of MSLP within 3×3 grid points, and defined cyclone size as the distance between these local minima and

the nearest MSLP saddle point. In both reanalyses, about 40% of cyclones have radii between 500 – 1000 km. The average radius is about 1000 km based on ERA-15, and about 900 km based on NCEP reanalyses. Using NCEP-NCAR reanalyses, Rudeva and Gulev (2007) and Rudeva and Gulev (2011) defined effective cyclone radius as the distance from the low-pressure centre to the point, at which the radial derivative of MSLP goes to zero. They found that effective radii varied between 200 – 1000 km, with 50% of radii between 400 – 800 km.

Based on these results, a low-pressure centre is identified here as any MSLP minimum within a moving circular window of 1000 km radius. Contrary to using a fixed number of grid points, the constant physical size of the test window takes into account grid-point convergence towards higher latitudes. The identified minima are closed in the sense that, with pressure rounded to nearest tenth hectopascal, the minimum value is only found at directly adjacent grid points within the test window. If the same minimum value occurs at neighbouring grid points, that grid point is chosen with the largest mean radial MSLP gradient within 1000 km. Following the consensus of previous studies (e.g., Raible, Della-Marta, Schwierz, Wernli, & Blender, 2008; Schneidereit, Blender, Fraedrich, & Lunkeit, 2007; Serreze, 1995), to avoid uncertainties associated with projecting surface air pressure to mean sea level, especially over Greenland, only MSLP minima are considered here, if the local terrain elevation does not exceed 1000 mASL.

Then, to be able to focus on well-developed storm systems, the number of relevant low-pressure centres is limited based on their intensity. Over the years, different measures of the intensity of low-pressure centres have been defined. One of the oldest measures is the absolute value of the pressure minimum. For local analyses, this may be appropriate. However, over a large area, as in this study, the use of central pressure for the comparison of cyclone intensity is problematic, due to the spatial variability in the background pressure field. Another common approach is to use pressure tendency at the cyclone centre. However, this is a measure of the intensity of cyclone development, rather than the intensity of fully developed cyclones, which are the focal point of this study. An indication of the large-scale impact of a well-established cyclone is more appropriately given by the average radial pressure gradient around the low-pressure centre, which is directly related to the tangential wind speed, and therefore to the actual circulation. This also avoids the problem of grid-point convergence towards the poles, that affects the calculation of centre depression, relative to the surrounding grid points.

Therefore, the intensity of low-pressure centres is defined here as the average (first order) radial MSLP gradient within 1000 km of a given local MSLP minimum (similar to the methodology employed by Blender et al. (1997), Blender and Schubert (2000), Schneidereit et al. (2007), and Raible et al. (2008)). The resulting pressure gradient is multiplied by half the maximum distance (500 km), to give half-width depression. Only those low-pressure centres are included in the analysis, for which half-width depression is at or above the 25th percentile of all local minima within a given season. These low-pressure centres are then considered intense enough to be referred to as "cyclones". In the case of daily time-series, or daily time-series smoothed by 5-day running means, these cyclones can be interpreted as actual storm systems. In the case of 31-day running means, the longer-term depressions are more indicative of persistent storm activity within that region.

For daily averages, minimum values for half-width depressions are 6.53 hPa in winter, and 4.25 hPa in summer. Across the study domain, this results in an average of 1.7 cyclones identified per day in winter, and 2.0 cyclones per day in summer.

5 Spatial distribution of cyclone centres

When determining the areal density of the long-term spatial distribution of cyclone centres, the area represented by each model grid point must be taken into account. At latitude ϕ, the grid-box size is given by

$$dA = \bar{a}^2 \cos\phi \, d\lambda \, d\phi \,, \tag{1}$$

where $\bar{a} = 6371$ km is the Earth's mean radius, and latitude and longitude are measured in radians. For the ECMWF reanalyses, angular grid-point spacing $d\lambda = d\phi = \pi/180$ is constant across the domain. The low-pressure centre count at each grid point is then multiplied by $\overline{dA}/dA$, with mean grid-point area $\overline{dA}$, to give a spatially uniform measure of the seasonal occurrence of cyclones.

Cyclone density calculated in this fashion is purely based on the spatial distribution of a collection of instantaneous low-pressure centres, rather than storm tracks. A high count of low-pressure centres in a particular region may therefore be the result of the frequent passage of fast-moving cyclones, or a smaller number of slow-moving cyclones. Tracking of cyclone centres would require the determination of distinct low-pressure centres, and would therefore depend on the specification of additional subjective criteria. For the climatological analyses in this study this is unnecessary, since the chronological order of identified cyclone centres (whether a low-pressure centre evolved from an earlier one, or is a different storm system) is irrelevant.

For daily averages, as well as 5-day and 31-day running means, this is shown in Figure 7. In winter, the region with the highest cyclone density – associated with frequent or persistent occurrence of individually identifiable cyclonic storm systems, forming in, or moving into the region – is found between Iceland and the southern tip of Greenland, which is consistent with earlier findings (e.g., Dacre & Gray, 2009; Hanson et al., 2004; Hodges, Lee, & Bengtsson, 2011; Jahnke-Bornemann & Brümmer, 2009; Raible et al., 2008; Schneidereit et al., 2007; Serreze et al., 1993; I. F. Trigo, 2006; Wang, Swail, & Zwiers, 2006; Wernli & Schwierz, 2006). Therefore, whether defined as a local minimum of the seasonal mean MSLP field, or a region with intense cyclone activity, the Icelandic Low is a robust feature of the North Atlantic climate system, qualitatively independent of differences in the datasets used, the study period, or the cyclone identification method. Also consistent with the earlier findings, other regions with a high wintertime cyclone occurrence are located over the Norwegian and Barents seas, as well as southwest of Greenland and over Baffin Bay. Over land, wintertime low-pressure centres with depressions above the 25th percentile are rare compared with maritime storm systems. In summer, cyclones are distributed more widely, including the land areas.

While there is agreement about the relative distribution of cyclones, the absolute number of identified daily low-pressure centres not only depends on the specific numerical criteria and threshold values of the identification scheme, but also on the resolution of the pressure data. Higher spatial resolution results in a higher number of identified cyclones, with deeper cores and longer tracks (Hanson et al., 2004; Hodges et al., 2003, 2004, 2011; Raible et al., 2008; I. F. Trigo, 2006; Ulbrich et al., 2009; Wang et al., 2006). For the criteria used in this study,
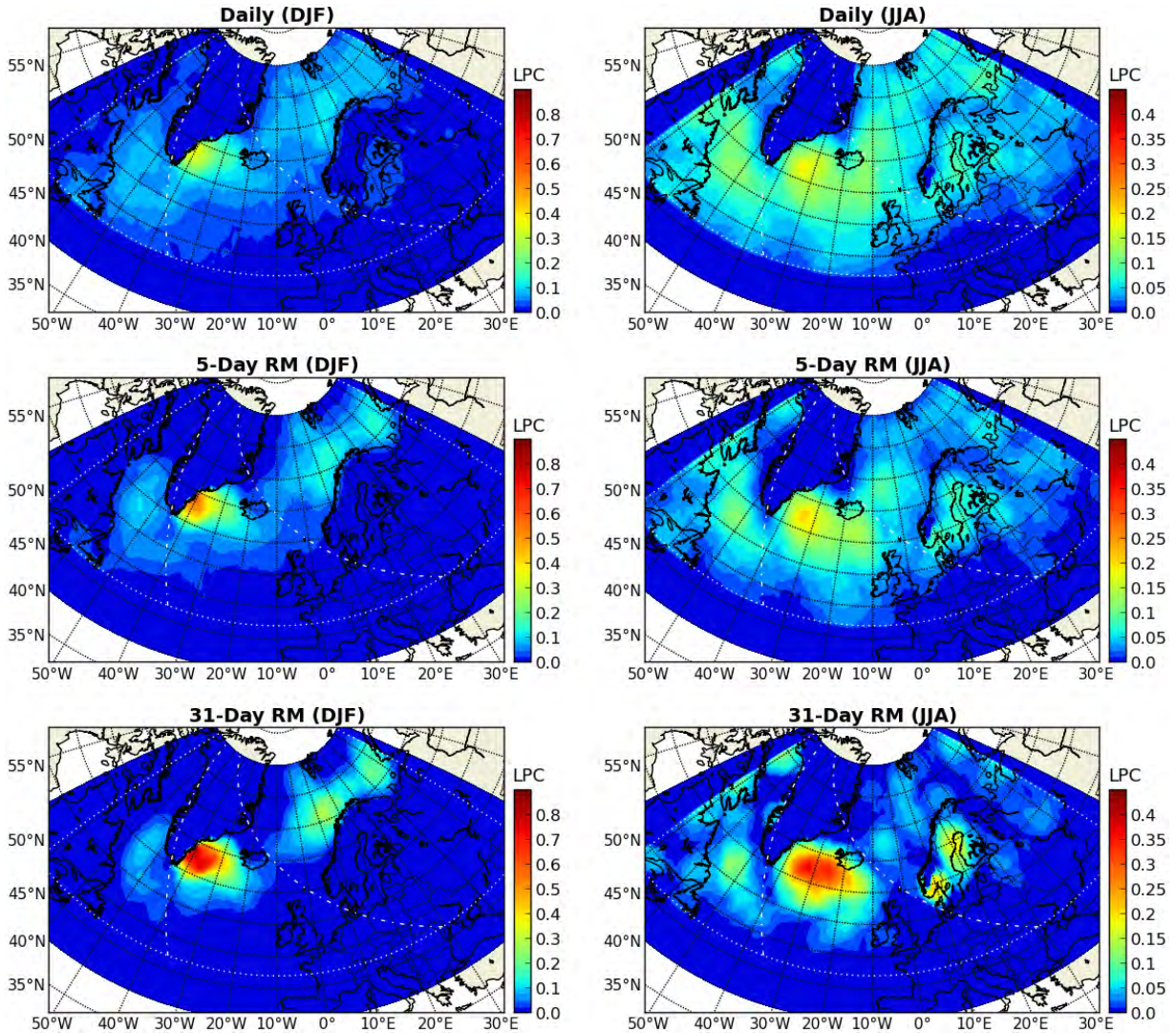
Figure 7. Seasonal per grid point occurrence of low-pressure centres (LPC) for daily averages, as well as for 5-day and 31-day running means of daily grid-point time-series. The dotted lines indicate the domain boundaries. The dash-dotted lines indicate boundaries between different sectors, as described in the text. Note the difference in scale of the colour shading between winter and summer.

based on daily averages, the total number of cyclones per season is 135 (142) in winter (summer) over the ocean, and 20 (47) in winter (summer) over land. As shown in more detail in Figure 8, over the ocean, there is a shift to more intense storm systems from summer to winter, with a 5% decrease in the overall number of identified cyclones. Over the land, the number of cyclones increases by a factor of 2.4 from winter to summer, primarily by an increase in the occurrence of below average depressions, relative to the wintertime distribution. In winter, there are 6.8 times more cyclones occurring over the ocean than over the land. In summer, that ratio is reduced to 3.0. However, throughout the year, cyclones over the ocean are not only more frequent, but also on average more intense than over land.
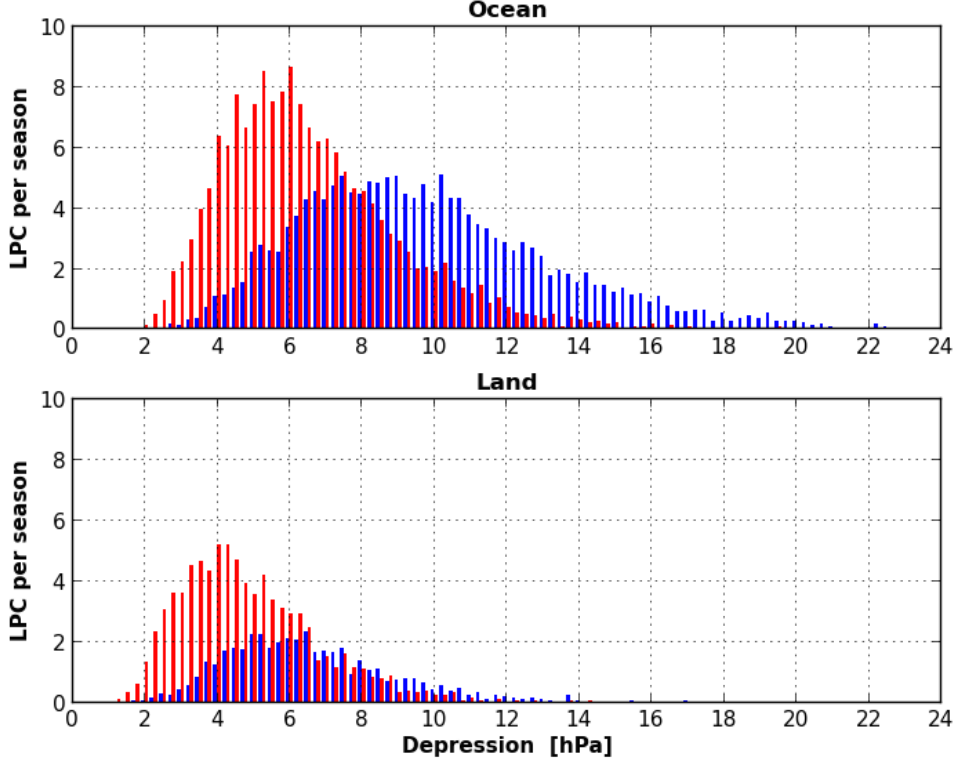
17

Figure 8. Occurrence of low-pressure centres, as a function of centre depression, per winter (blue bars) and summer (red bars) season over the entire ocean or land area within the study domain.

As shown in Figure 7, increasingly with longer time-scales, cyclones tend to cluster in three preferred regions within the study domain, with a low occurrence of MSLP minima at the boundaries. With longitude, λ, parameterised as a function of latitude, ϕ, these boundaries are at

$$\lambda_1 = -30 - \frac{30}{40}(\phi - 40) \tag{2}$$

and

$$\lambda_2 = 45 - \frac{90}{40}(\phi - 40) \ . \tag{3}$$

This suggests dividing the study domain into three parts: a western sector, with $\lambda < \lambda_1$, covering the region west of Greenland; a central sector, with $\lambda_1 \leq \lambda < \lambda_2$, including the region of the Icelandic Low; and an eastern sector, with $\lambda \geq \lambda_2$, containing the region with frequent cyclone activity to the northeast of Iceland. Then, of the total study area, 22% fall into the western sector (itself broken up into 70% ocean and 30% land), 32% in the central sector (77% ocean, 23% land), and 46% in the eastern sector (44% ocean, 56% land).

The average seasonal cyclone occurrences over the ocean and land areas in different sectors are listed in Table 1. For daily time-series in winter, the uniform spread of storm systems over the ocean in the eastern sector results in the highest average cyclone density, compared with other ocean areas. Otherwise, the highest density of maritime storms is found in the central sector. With longer time-scales, cyclone density over the ocean further increases in the central sector, while decreasing over the other maritime regions. Simultaneously, the percentage of continental

Table 1. Seasonal cyclone density [cyclones per season per 1000 km × 1000 km] over the ocean / land areas in different sectors, for daily averages, as well as for 5-day and 31-day running means (RM) of daily grid-point time-series. Percentages measure cyclone density over land relative to that over the ocean.

Time-Series	West	Central	East
Daily (DJF)	8.7 / 3.2 (37%)	10.8 / 1.2 (11%)	11.6 / 2.6 (22%)
Daily (JJA)	10.0 / 7.2 (72%)	11.9 / 2.6 (22%)	9.4 / 5.9 (63%)
5-Day RM (DJF)	6.2 / 0.8 (13%)	10.8 / 0.3 (3%)	9.9 / 0.7 (7%)
5-Day RM (JJA)	7.0 / 5.5 (79%)	10.7 / 2.0 (19%)	6.4 / 4.8 (75%)
31-Day RM (DJF)	3.2 / 0.0 (0%)	12.5 / 0.0 (0%)	9.7 / 0.0 (0%)
31-Day RM (JJA)	4.8 / 6.0 (125%)	11.4 / 1.4 (12%)	3.8 / 3.7 (97%)

relative to maritime storms decreases. This relative and absolute increase in the occurrence of maritime cyclones in the central sector, with increasing time-scale, emphasises again the climatological significance of the Icelandic Low. During summer, the cyclone density over land increases on all time-scales and in each sector, compared with winter. There is also a relative increase in cyclone density over land, compared with the maritime regions. However, with the exception of 31-day running means in the western sector (the Canadian maritime provinces and southern Baffin Island), absolute cyclone density over land remains lower than over the ocean, where summertime cyclone density increases in the western sector, but decreases in the east, with only small changes in the central sector.

In addition to changes in cyclone occurrence, there are also seasonal differences in the average cyclone intensity, or centre depression (see Table 2). As is to be expected, on all time-scales and across the study domain, wintertime average depressions are consistently greater than in summer, both over the ocean and over the land. Furthermore, cyclones are consistently more intense over the ocean than over land, with the largest average depressions occurring in the central sector. Due to the spatial smoothing, which is related to temporal averaging, average depressions decrease with time-scale.

Each large-scale MSLP field over the northern North Atlantic region can be characterised by the presence of cyclones in different combinations of the three distinct regions of enhanced cyclone

Table 2. Average seasonal centre depression [hPa] over the ocean / land areas in different sectors, for daily averages, as well as for 5-day and 31-day running means (RM) of daily grid-point time-series.

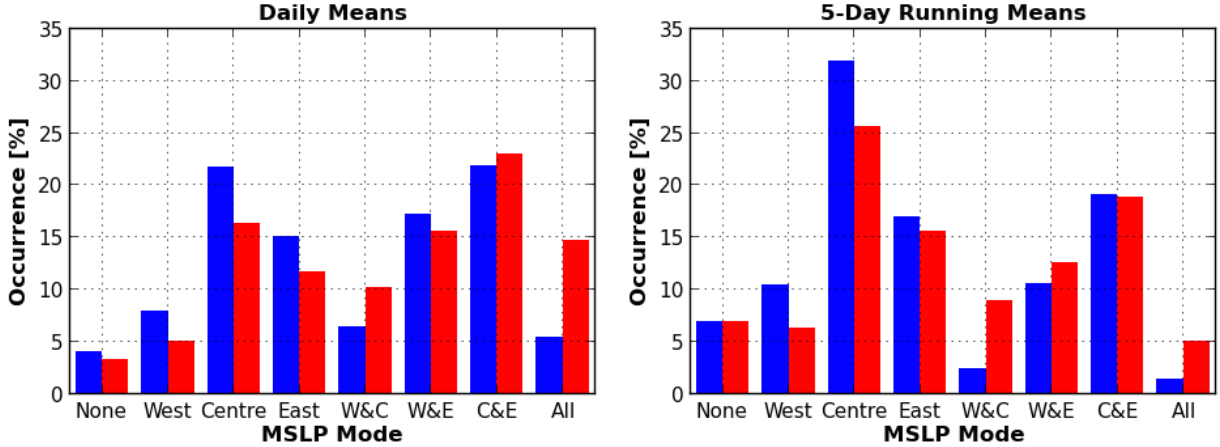| Time-Series	West	Central	East
Daily (DJF)	10.6 / 9.4	11.2 / 9.9	10.4 / 8.2
Daily (JJA)	6.8 / 6.1	7.5 / 6.6	6.9 / 6.1
5-Day RM (DJF)	6.0 / 5.7	7.2 / 6.7	6.3 / 5.0
5-Day RM (JJA)	4.0 / 3.6	4.6 / 3.9	4.1 / 3.6
31-Day RM (DJF)	3.5 / –	4.7 / –	3.7 / –
31-Day RM (JJA)	1.9 / 1.6	2.3 / 1.8	2.0 / 1.7

Figure 9. Relative occurrence of MSLP modes for daily averages, as well as for 5-day running means of daily grid-point time-series, in winter (blue bars) and summer (red bars).

activity. Eight modes of the MSLP field can then be defined: 1 mode without any significant cyclone in any sector, 3 modes with at least one cyclone in only one sector (West, Centre, East), 3 modes with simultaneous cyclones in two sectors (W&C, W&E, C&E), and 1 mode with cyclones in all three sectors. This classification scheme, in principle, amounts to empirical pattern recognition, based on large-scale weather systems, rather than a statistical data reduction approach to identifying a set of basic states, as in empirical orthogonal function (EOF) analysis. The different cyclone modes, as defined here, are physically recognisable states of the tropospheric circulation, and therefore have a more immediate physical interpretation than EOFs.

The relative seasonal occurrence of different MSLP modes is shown in Figure 9 for daily averages, as well as for 5-day running means. For daily means in winter, the most common modes with approximately equal occurrence of about 22% are the Centre and Centre-and-East (C&E) mode. In summer, as seen before, there is a shift towards a more widespread distribution of cyclones, with a decrease in the occurrence of no- or single-cyclone modes, and an increase in the occurrence of multiple-cyclone modes. Conversely, for 5-day running means, compared with daily means, there is an increase in the occurrence of no- or single-cyclone modes, primarily in the central sector.

This classification of large-scale MSLP fields into eight modes is complete, since every pressure field is accounted for. It is also unique, since no pressure field is counted twice. Therefore, in each season, the average field of all composite mean fields for individual modes, weighted by the modal occurrences shown in Figure 9, is equal to the seasonal mean field.

The eight modal mean MSLP fields, together with the corresponding average centred temporal tendencies of the MSLP field ($\delta p/\delta t|_{t_0} = (p(t_0 + \delta t) - p(t_0 - \delta t))/2\delta t$, with $\delta t = 2$ days) in winter are shown in Figure 10. In summer, the spatial patterns of mean MSLP fields are similar but less distinct, with weaker pressure tendencies (not shown). Based on the average pressure tendencies for different MSLP modes, in most scenarios, cyclones over the northern North Atlantic tend to move eastwards. However, pressure tendencies around a particular cyclone not only depend on the location of that cyclone, but also on the larger-scale MSLP pattern. Without significant low-pressure centres in other sectors, central cyclones tend to move northeast across

Iceland, bringing the island under the influence of a cold front, rather than warm air advection from the south, as is the case for approaching cyclones. With additional cyclones in the eastern sector, central cyclones tend to stay south of Iceland, whereas with additional cyclones in the western sector, there is a tendency for central cyclones to move west. This is also the case with cyclones in all three sectors. Cyclones in the eastern or western sector are also strongly affected by the presence of central cyclones. In both sectors, cyclones tend to move east, unless there are cyclones in the neighbouring sector, in which case pressure tendencies are reversed.
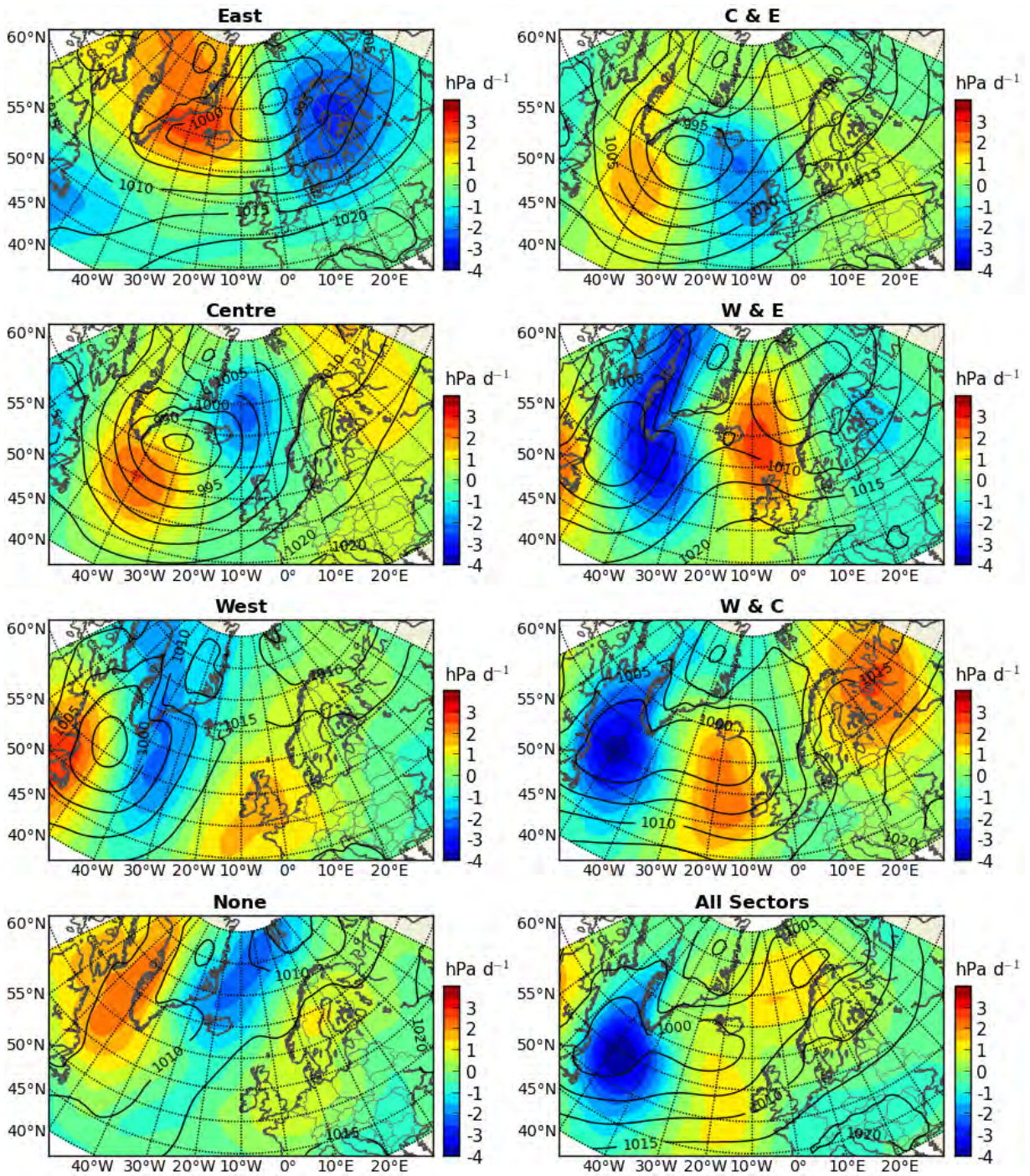
Figure 10. Composite mean temporal MSLP tendencies, for different MSLP modes. Composite mean MSLP in hectopascals is shown by the black contours.

6 Upper-level flow associated with different MSLP modes

In this section, planetary waves and their significance for mid- and upper-level forcing (within the troposphere) of surface low-pressure centres and cyclones will be discussed. To determine differences in the large-scale tropospheric circulation, which are associated with well-developed low-pressure centres in the three preferred regions that were discussed in the previous section, wintertime composite mean fields of geopotential height at 500 and 250 hPa for different MSLP modes are shown in Figure 11, together with the associated mean 500 hPa height anomalies. These anomalies are defined as deviations of daily fields from the seasonal mean field in each year. This eliminates differences in average anomalies for different MSLP modes, that are due to interannual variations in seasonal means, combined with interannual differences in the relative occurrence of MSLP modes, and are therefore not related to the spatial variability of the MSLP field. The composite mean fields between the first (1979 – 94) and the second half (1995 – 2010) of the study period are qualitatively the same (not shown), suggesting that the average waves and spatial patterns of anomalies are statistically robust. Also, the same prevailing waves and spatial patterns are found in summer, but with reduced magnitudes (not shown).

The pattern of 500 hPa geopotential height anomalies associated with the East mode is similar to the negative East Atlantic pattern, identified by Handorf and Dethloff (2012) based on an EOF analysis of ERA-40 data, for the winters (DJF) during the 1958 – 1999 period. The northeast-to-southwest anomaly gradient across the northern North Atlantic accompanies a strong polar vortex, with weak meridional but strong westerly flow at mid- and upper-levels across the ocean and into Western Europe. The no-cyclone mode is similar to the negative North Atlantic Oscillation (NAO) phase, with a southeast-to-northwest 500 hPa geopotential height anomaly gradient.

Aside from these two phenomenological cyclone-based MSLP modes, there is no close correspondence to any of the wintertime height anomaly patterns based on EOF analysis. A positive NAO phase is often seen as being indicative of a strong Icelandic Low. However, as seen in Figure 11, the composite 500 hPa geopotential height anomaly pattern, associated with intense cyclones exclusively located within the region of the climatological Icelandic Low, is rotated by about 90 degrees relative to a positive NAO pattern. The Centre-and-East (C&E) mode is associated with height anomalies that would result in a positive NAO index. However, the larger-scale circulation supporting this mode is different from that of a positive NAO pattern (compare again with Handorf and Dethloff (2012)).

The Centre and West-and-East (W&E) modes are associated with opposite mid-level geopotential height anomaly patterns within the study domain. The Centre mode is forced by an anomalously strong jet streak and deep mid-level trough, with an axis oriented towards the southeast from the southern tip of Greenland. As such, it is shifted eastwards from its seasonal mean position over the Labrador Sea (see again Figure 3). Cyclones in the central sector therefore preferably form underneath the left exit region of the composite mean jet streak (compare with Figure 7 in the previous section), consistent with the well-established role played in cyclone development by positive vorticity advection and upper level divergence. By contrast, during the W&E mode, the planetary wave pattern over the northern North Atlantic is shifted slightly westwards relative to the seasonal mean position, with a ridge over the central sector, and a trough over eastern Scandinavia. Consequently, as for the Centre mode, surface cyclones form underneath the left exit region of the composite mean jet streak.

23

The C&E mode mainly differs from the Centre mode by the absence of positive geopotential height anomalies over Scandinavia, with slightly weaker negative anomalies over the central sector. However, cyclones associated with this mode are also forced by an anomalously strong jet streak and deep mid-level trough.

The main difference of the W&E mode, compared with the West mode, is the greater extent of negative geopotential height anomalies over the European continent, and especially over Scandinavia, with a slight weakening of the mid-level planetary wave pattern over the western part of the domain.

For the West-and-Centre (W&C) mode, cyclone activity in the two sectors is separated by weakly positive geopotential height anomalies over the western North Atlantic.

Similar to eastern cyclones, the MSLP mode with significant cyclones in all sectors is associated with a strong polar vortex, with weak meridional but strong westerly flow at mid- and upper-levels.
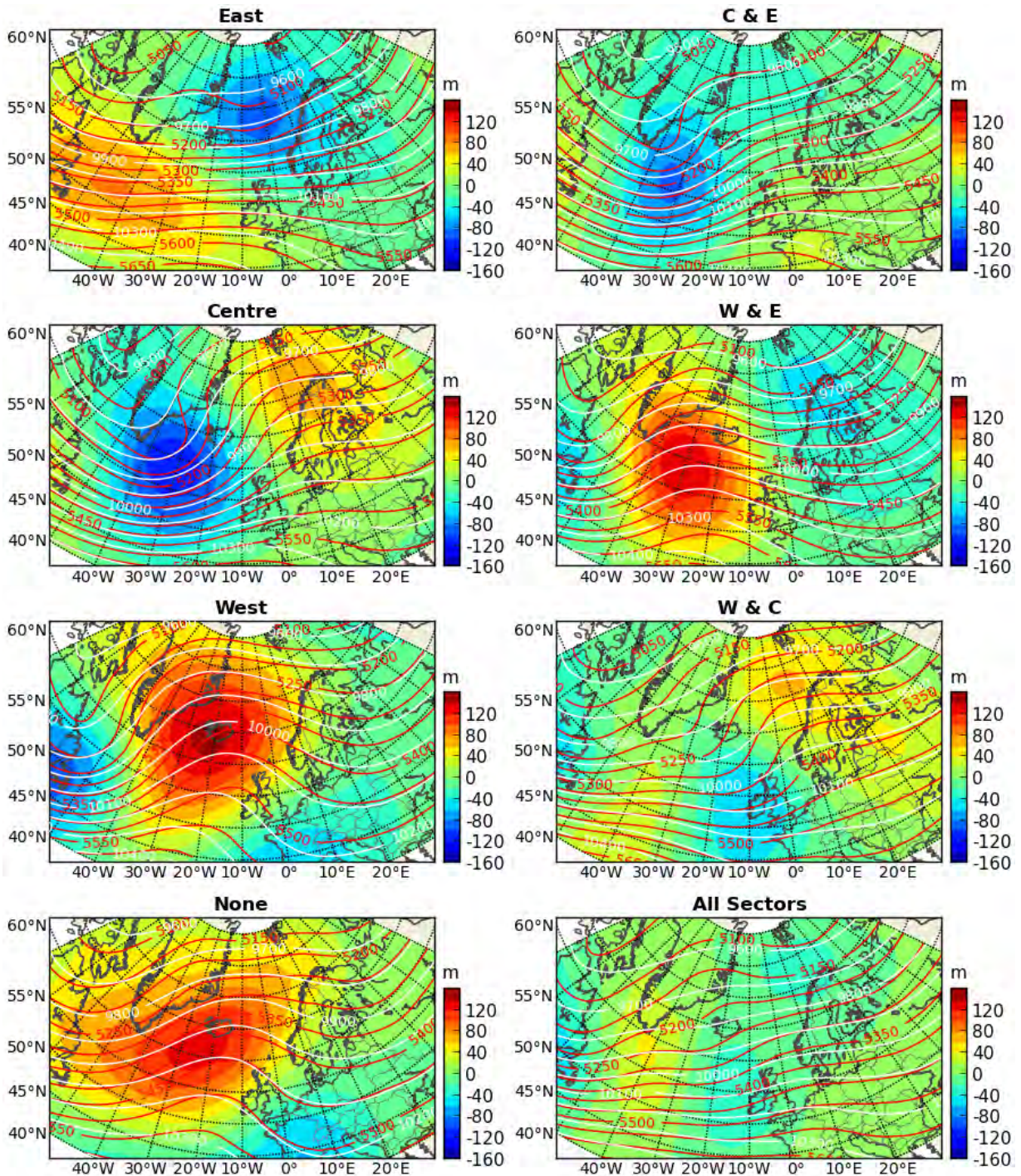
Figure 11. Composite mean anomalies of 500 hPa geopotential height, for different MSLP modes. Also shown are composite means of geopotential height in metres at 500 hPa (red contour lines) and 250 hPa (white contour lines).

7 Weather anomalies associated with different MSLP modes

The connection between local temporal fluctuations of MSLP and other atmospheric surface variables, on time-scales of a few days, was discussed in Section 3. In this section, the effects of different spatial patterns of the MSLP field, and thus of horizontal pressure gradients, on atmospheric surface variables will be analysed; specifically, spatial anomalies of wind, temperature, and precipitation. As in the previous section, anomalies are defined as deviations of daily fields from the seasonal mean field in each year.

A large number of studies have investigated the impact of different phases of the Arctic and North Atlantic Oscillations on surface weather conditions across the North Atlantic region, including Greenland and western Europe (e.g., Handorf & Dethloff, 2012; Hurrell, 1995; Hurrell & Deser, 2009; Hurrell & van Loon, 1997; Rogers, 1997; Schneidereit et al., 2007; Serreze et al., 1997; Skeie, 2000; R. M. Trigo et al., 2008; van Loon & Rogers, 1978; Wu, Wang, & Walsh, 2006). They have consistently shown that even relatively small changes in the large-scale prevailing circulation, characterised by changes in the NAO index, can have a significant impact on the seasonal climatic conditions across western Europe. During a positive NAO phase, the axis of maximum moisture transport and enhanced precipitation over the eastern North Atlantic shifts from the west-northwesterly direction it has during a negative phase, to a more southwesterly direction, extending farther north across Iceland and into northern Europe. Despite generally enhanced storm activity over the northern North Atlantic, the shift in moisture transport results in reduced precipitation over southern Europe and the Mediterranean. Connected to the enhanced moisture transport into northern Europe are anomalously high surface air temperatures, while southern Europe is unseasonably cold.

Jahnke-Bornemann and Brümmer (2009) studied the impact of changes in the large-scale circulation across the Nordic Seas on surface air temperature and sea ice concentration. To characterise the MSLP field in that region, they used an index analogous to the NAO index introduced by Hurrell (1995), referred to in the paper as ILD index. It is calculated as the difference between normalised pressure anomalies measured at the approximate centre of the Icelandic Low, and at the highest concentration of low pressure centres north of the Lofoten Islands. With simultaneously positive or negative anomalies at the two reference points, large-scale MSLP anomalies are consistent with negative or positive NAO patterns, respectively. For alternating anomalies, high pressure in the region of the Icelandic Low, combined with low pressure north of the Lofoten, leads to enhanced northwesterly flow, low surface air temperatures over the ocean east of Greenland and over western Europe, together with high temperatures south of Greenland and over eastern Europe.

As discussed in the previous section, there is generally no close correspondence between the MSLP modes introduced here, and the teleconnection patterns based on EOF analysis. Focussing more on the northern North Atlantic region, the pattern of 500 hPa geopotential height anomalies shown in Figure 11 for the Centre and East modes is very similar to the MSLP anomalies derived by Jahnke-Bornemann and Brümmer (2009) for positive or negative ILD indices, respectively. However, as seen previously, the mid- and upper-level circulation patterns, and therefore potentially surface weather anomalies, differ significantly if MSLP anomalies in either the central or eastern sector occur simultaneously with anomalies in the western sector.
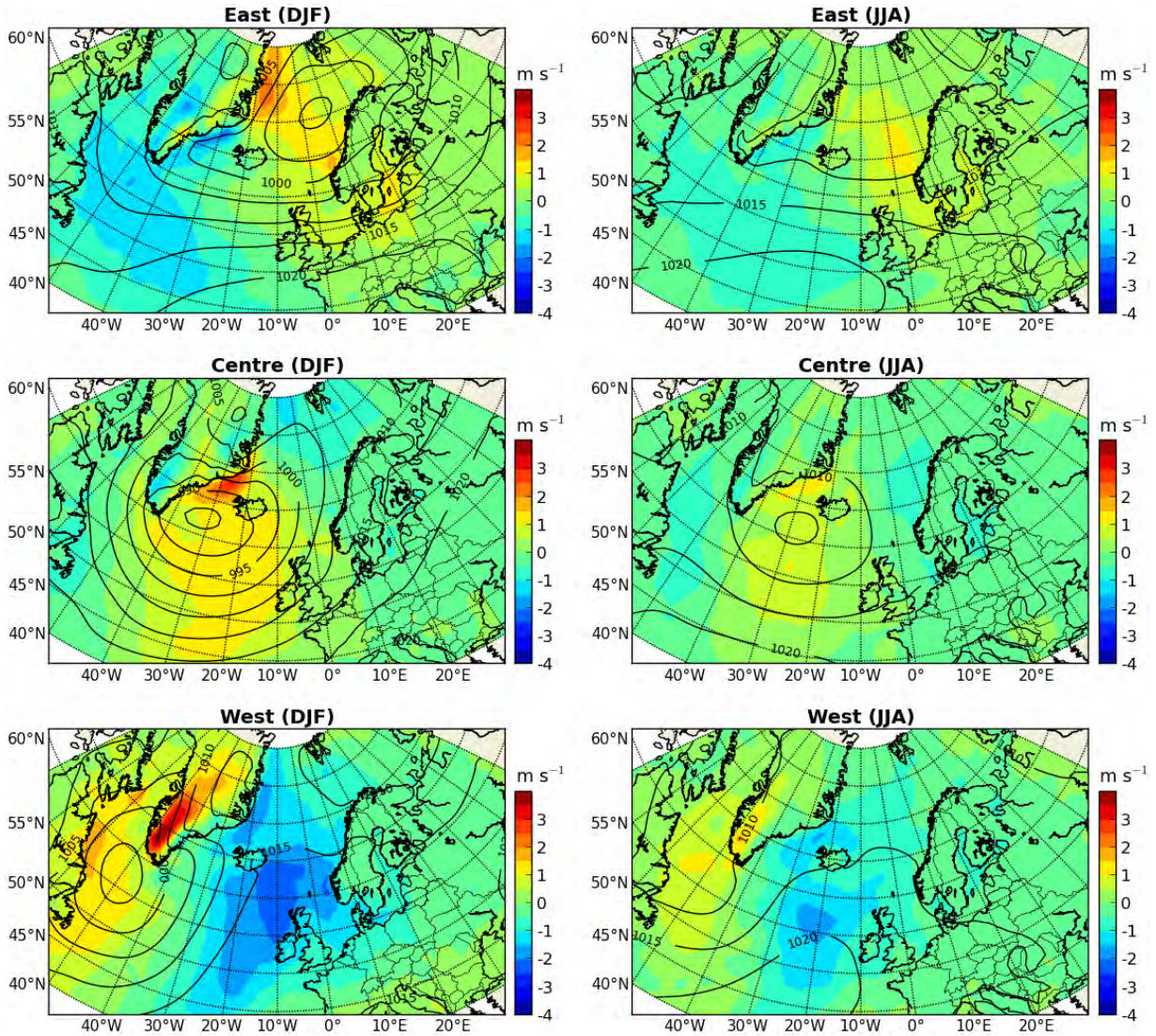
Figure 12. Composite mean fields of daily surface wind speed anomalies in winter and summer, for different MSLP modes. Composite mean MSLP in hectopascals is shown by the black contours.

The composite mean fields of daily surface wind speed anomalies in winter and summer, for different MSLP modes, are shown in Figure 12. In the interest of brevity, the discussion is limited to situations with well-developed cyclones in only one of the three sectors. For 5-day running means, anomalies qualitatively display the same pattern, but with smaller magnitudes (not shown). In winter and summer, the largest positive anomalies of wind speed over the ocean are found in the sector with the lowest mean pressure. However, with cyclones in the western sector, strong enhancement compared to the seasonal mean also occurs for southerly flow over Greenland. Despite a weaker large-scale circulation in summer, the spatial patterns of positive and negative anomalies in winter and summer are qualitatively the same. With cyclones in the eastern sector, the large positive anomalies along the northeast coast of Greenland are the result of an enhanced pressure gradient between the low-pressure over the ocean, and the prevailing high pressure over Greenland. With most eastern cyclones situated in the northern part of the
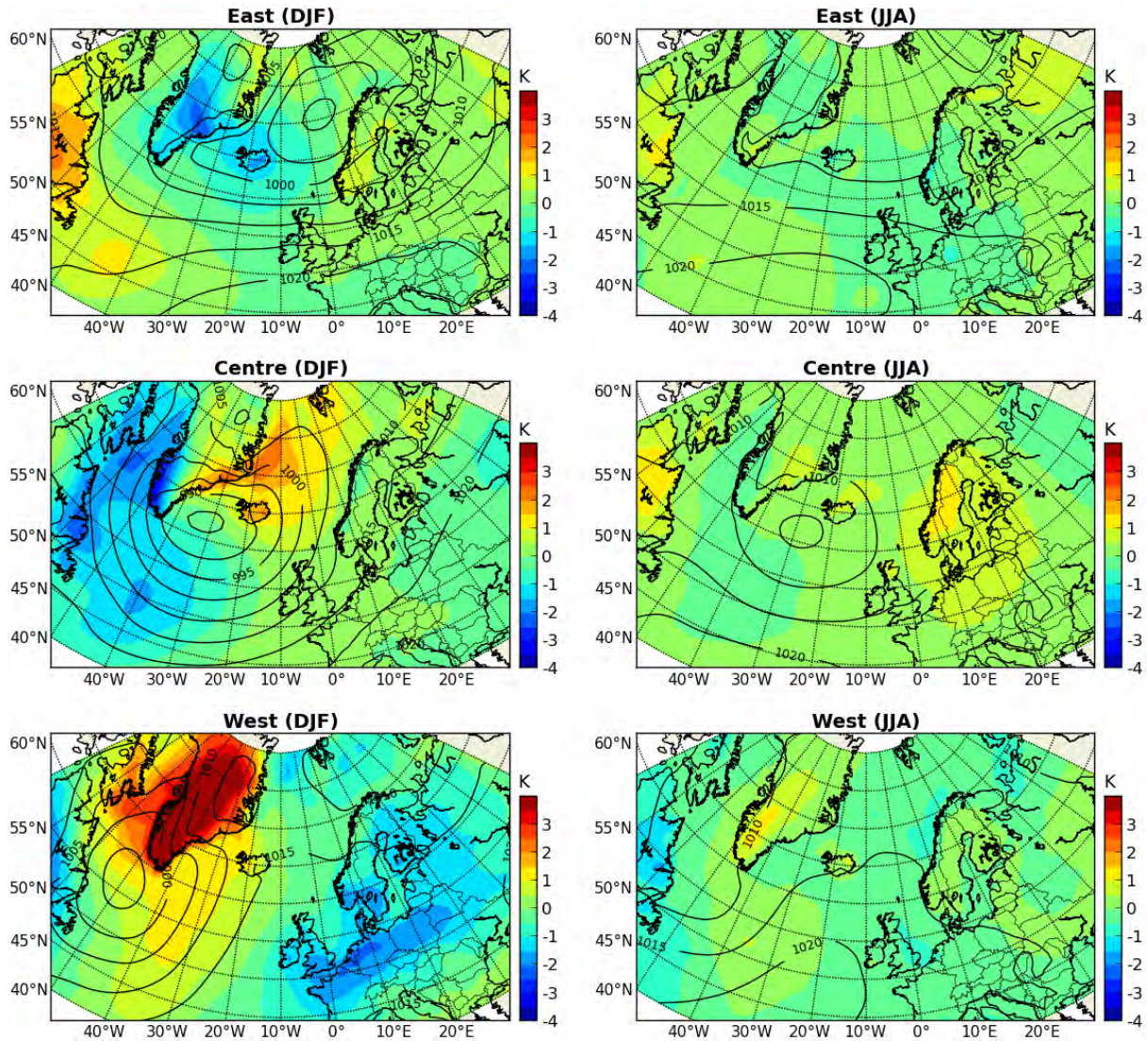
Figure 13. Composite mean fields of daily surface air temperature anomalies in winter and summer, for different MSLP modes. Composite mean MSLP in hectopascals is shown by the black contours.

domain, the enhanced westerlies over northwest Europe are due to the intensification of the prevailing north – south pressure gradient across the polar front. The opposite is true for cyclones in the western sector. For cyclones in the central sector, the prevailing seasonal pressure gradients (and therefore winds) are intensified relative to the higher pressure in the south and over Greenland, but weakened relative to the lower pressure in the northeast. For Iceland, the main difference exists between the West and Centre mode, with anomalies of -1 m s^{-1} and 1 m s^{-1}, respectively.

The analogous results for surface air temperature are shown in Figure 13. As for wind speed, the magnitudes of summertime temperature anomalies are small compared with winter. Additionally, however, there are significant qualitative differences. These are due to seasonal changes in land–sea temperature contrasts. In winter, the anomaly pattern with warm (cold) temperatures over northern (southern) Europe, which is often attributed to a positive NAO phase, is associ-
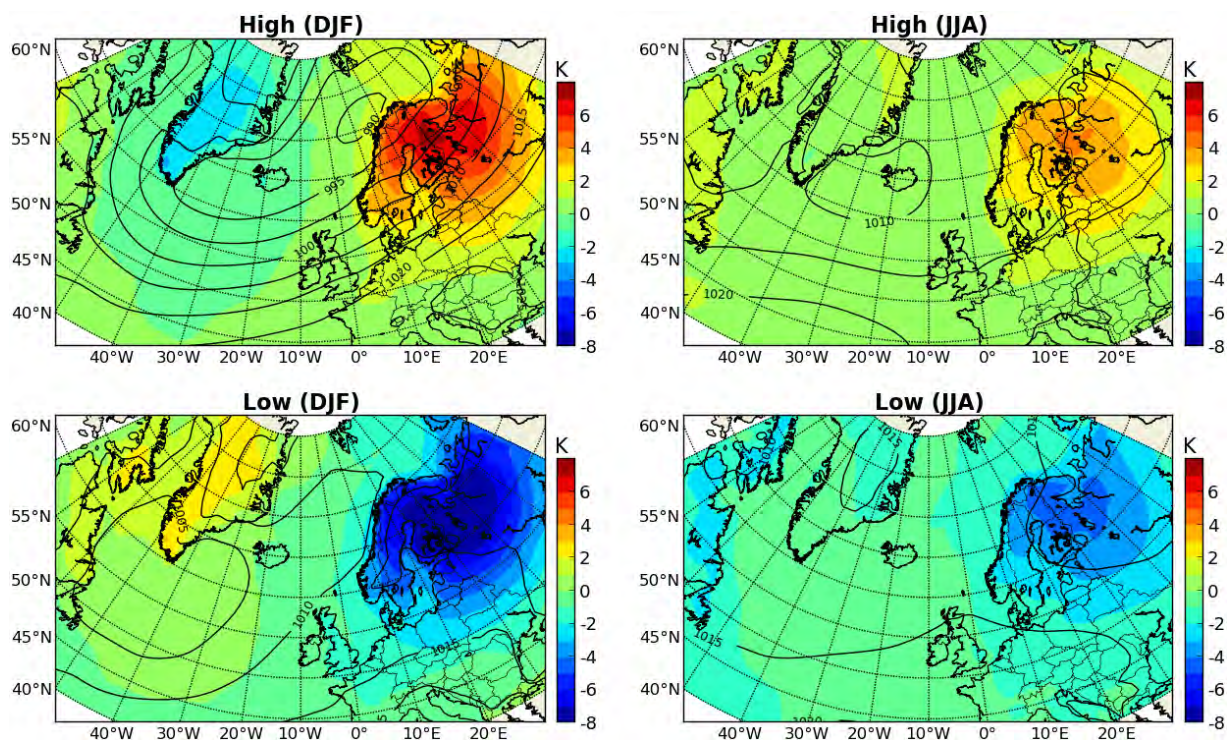
Figure 14. Composite mean fields of daily surface air temperature anomalies in winter and summer, for high or low regional temperatures over Scandinavia. Composite mean MSLP in hectopascals is shown by the black contours.

ated with cyclones in the eastern sector, whereas for cyclones in the central sector, temperature anomalies across Europe are small, and slightly negative along the Norwegian coast. With cyclones in the western sector, high pressure settles over the European continent, leading to anomalously low wintertime temperatures. Since most cyclones in the central sector occur southwest of Iceland, whereas most cyclones in the eastern sector occur towards the northeast, a transition between the Centre and East modes results in a switch between southerly and northerly winds over the island, and therefore a transition between positive and negative temperature anomalies.

As a reverse test of the connection between large-scale MSLP patterns and local variations in temperature, Figure 14 shows average surface air temperature anomalies in winter and summer, together with the corresponding mean MSLP fields, for high or low average temperatures over the land area of the Scandinavian Peninsula, where temperature extremes are defined to be within the highest or lowest 20th percentile of all regional averages within a given season. Qualitatively, the same results are obtained for extreme temperatures specified over Greenland (not shown). In winter, as for the classification of fields based on MSLP patterns, there is a well-defined dipole pattern in temperature anomalies between Greenland and northwest Europe. Warm Greenland temperatures are associated with average low pressure in the western and central sectors, whereas cold Greenland temperatures result if large-scale storm activity shifts northeastwards. The warmest temperatures over Scandinavia are related to an increased occurrence of low-pressure systems over the northern part of the Norwegian Sea, rather than a particularly intense Icelandic Low. In fact, compared with the seasonal mean pressure in the northeastern region of enhanced cyclone activity, the relative intensity of the Icelandic Low is weak during
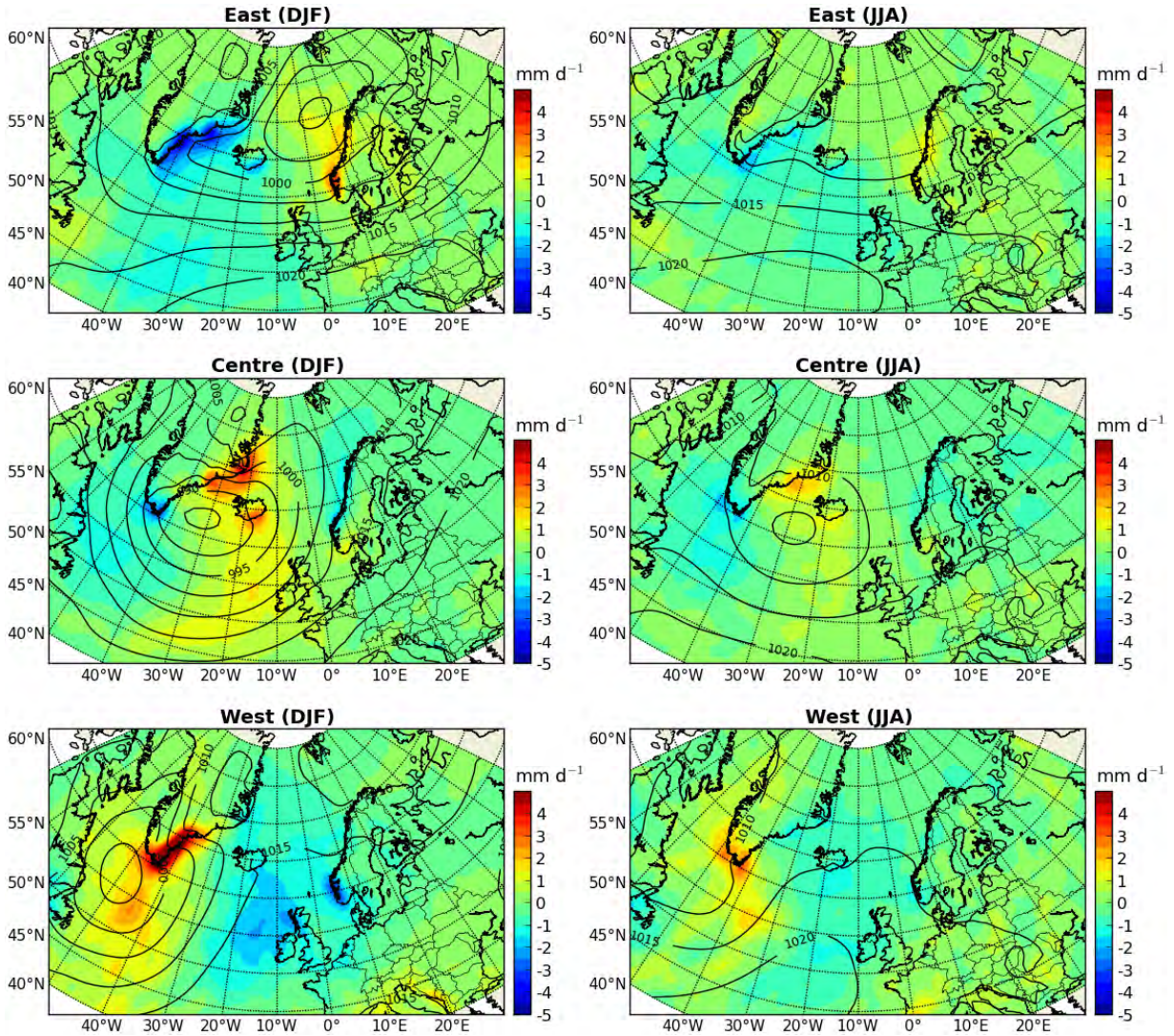
29

Figure 15. Composite mean fields of daily precipitation anomalies in winter and summer, for different MSLP modes. Composite mean MSLP in hectopascals is shown by the black contours.

warm spells affecting northern Europe. In summer, cyclones and large-scale temperature advection are weaker than during winter. Consequently, the well-defined dipole pattern in temperature anomalies between Scandinavia and Greenland is absent. Instead, surface air temperatures tend to vary in unison across the northern transatlantic region.

The composite mean fields of daily precipitation anomalies in winter and summer, for different MSLP modes, are shown in Figure 15. Despite reduced magnitudes in summer, the spatial pattern of positive and negative anomalies is qualitatively the same as in winter. The largest precipitation anomalies for different MSLP modes are related to forced ascent, either at air mass boundaries, or over elevated terrain. With cyclones in the eastern sector, enhanced westerlies over the warm waters of the Norwegian Sea (see again Figures 3 and 12) create large positive precipitation anomalies in combination with the elevated terrain along the southern coast of Norway. There are corresponding negative anomalies along the southeast coast of Greenland

and Iceland due to weaker coastal winds and advection of cold air masses from the north (see again Figure 13). The pattern reverses for cyclones in the western sector, as warm maritime winds from the south are forced to rise over the southern tip of Greenland, while over northwest Europe winds are weak. With cyclones in the central sector, the positive anomalies southeast of the composite low-pressure centre are due to warm air being lifted by the approaching cold front.

8 Summary

The short-term as well as seasonal weather conditions over Iceland and across Northwest Europe strongly depend on the location and intensity of dominant low-pressure centres over the northern North Atlantic and Nordic Seas.

A low-pressure centre is identified in this study as any closed local mean sea level pressure (MSLP) minimum within a moving circular window of 1000 km radius. The intensity of low-pressure centres is measured by half-width depression, defined as the average radial MSLP gradient within 1000 km of a given local minimum, multiplied by 500 km. Only those low-pressure centres are taken into account, for which half-width depression is at or above the 25th percentile of all local minima within a given season. These low-pressure centres are then considered intense enough to be referred to as cyclones.

In winter, the region with the highest cyclone density is found between Iceland and the southern tip of Greenland. Other regions with a high wintertime cyclone occurrence are located over the Norwegian and Barents seas, as well as southwest of Greenland and over Baffin Bay.

This suggests dividing the study domain into three sectors, corresponding to the three distinct regions of enhanced cyclone activity: a western sector, covering the region west of Greenland; a central sector, including the region of the Icelandic Low; and an eastern sector, containing the region with frequent cyclone activity to the northeast of Iceland. Each large-scale MSLP field within the study domain can then be characterised by the presence of cyclones in different combinations of sectors, and classified as belonging to one of eight modes.

Generally, there is no close correspondence between these phenomenological cyclone-based MSLP modes and any of the dominant teleconnection patterns based on empirical orthogonal function analysis. A positive phase of the North Atlantic Oscillation (NAO) is often seen as being indicative of a strong Icelandic Low. However, the composite 500 hPa geopotential height anomaly pattern, associated with intense cyclones exclusively located within the central sector, is rotated by about 90 degrees relative to a positive NAO phase. The wintertime anomaly pattern with warm (cold) temperatures over northern (southern) Europe, which is often attributed to a positive NAO phase, is associated with cyclones in the eastern sector, whereas for cyclones in the central sector, temperature anomalies across Europe are small, and slightly negative along the Norwegian coast. With cyclones in the western sector, high pressure settles over the European continent, leading to anomalously low wintertime temperatures. The warmest temperatures over Scandinavia are related to an increased occurrence of low-pressure systems over the northern part of the Norwegian Sea, rather than a particularly intense Icelandic Low. In fact, compared with the seasonal mean pressure in the northeastern region of enhanced cyclone activity, the relative intensity of the Icelandic Low is weak during warm spells affecting northern Europe. In summer, cyclones and large-scale temperature advection are weaker than during winter. Con-

sequently, the well-defined dipole pattern in temperature anomalies between Scandinavia and Greenland is absent. Instead, surface air temperatures tend to vary in unison across the northern transatlantic region.

The largest precipitation anomalies for different MSLP modes are related to forced ascent, either at air mass boundaries, or over elevated terrain. With cyclones in the eastern sector, enhanced westerlies over the warm waters of the Norwegian Sea create large positive precipitation anomalies in combination with the elevated terrain along the southern coast of Norway. There are corresponding negative anomalies along the southeast coast of Greenland and Iceland due to weaker coastal winds and advection of cold air masses from the north. The pattern reverses for cyclones in the western sector, as warm maritime winds from the south are forced to rise over the southern tip of Greenland, while over northwest Europe winds are weak. With cyclones in the central sector, the positive anomalies southeast of the composite low-pressure centre are due to warm air being lifted by the approaching cold front.

The Centre and West-and-East (W&E) modes are associated with opposite mid-level geopotential height anomaly patterns within the study domain. The Centre mode is forced by an anomalously strong jet streak and deep mid-level trough, with an axis oriented towards the southeast from the southern tip of Greenland. As such, it is shifted eastwards from its seasonal mean position over the Labrador Sea. By contrast, during the W&E mode, the planetary wave pattern over the northern North Atlantic is shifted slightly westwards relative to the seasonal mean position, with a ridge over the central sector, and a trough over eastern Scandinavia. Different preferred regions of surface cyclone development are therefore activated by relatively small shifts in the mid- and upper-level tropospheric circulation.

The surface weather conditions across the northern North Atlantic region are significantly affected by these shifts, through the formation of cyclones in different sectors. This is particularly noticeable over Iceland, where a transition between MSLP modes (especially between the Centre and East modes) may lead to a reversal of the meridional component of the prevailing winds, and therefore the advection of different air masses. If in the context of climate change, a poleward shift in cyclone activity over the northern North Atlantic were to occur (as suggested recently by, for example, Wang et al. (2006), Ulbrich et al. (2009), and Wang et al. (2013)), the effects on regional temperatures over Iceland from an increased occurrence of northerly winds would counteract to some extent the general increase in surface air temperatures.

References

Anderson, D., Hodges, K. I., & Hoskins, B. J. (2003). Sensitivity of feature-based analysis methods of storm tracks to the form of background field removal. *Mon. Wea. Rev.*, *131*, 565-573.

Berrisford, P., Dee, D., Fielding, K., Fuentes, M., Kållberg, P., Kobayashi, S., & Uppala, S. (2009). *The ERA-Interim archive* (ERA Report Series No. 1). Reading, United Kingdom: European Centre for Medium Range Weather Forecast.

Bjerknes, J. (1919). On the structure of moving cyclones. *Mon. Wea. Rev.*, *47*(2), 95-99.

Bjerknes, J., & Solberg, H. (1922). Life cycle of cyclones and the polar front theory of atmospheric circulation. *Geofisiske Publikationer*, *III*(1), 3-18.

Blender, R., Fraedrich, K., & Lunkeit, F. (1997). Identification of cyclone-track regimes in the

North Atlantic. *Q. J. R. Meteorol. Soc.*, *123*, 727-741.

Blender, R., & Schubert, M. (2000). Cyclone tracking in different spatial and temporal resolutions. *Mon. Wea. Rev.*, *128*, 377-384.

Dacre, H. F., & Gray, S. L. (2009). The spatial distribution and evolution characteristics of North Atlantic cyclones. *Mon. Wea. Rev.*, *137*, 99-115.

Handorf, D., & Dethloff, K. (2012). How well do state-of-the-art atmosphere-ocean general circulation models reproduce atmospheric teleconnection patterns? *Tellus A*, *64*, 1-27.

Hanson, C. E., Palutikof, J. P., & Davies, T. D. (2004). Objective cyclone climatologies of the North Atlantic – a comparison between the ECMWF and NCEP reanalyses. *Climate Dyn.*, *22*, 757-769.

Hodges, K. I. (1994). A general method for tracking analysis and its application to meteorological data. *Mon. Wea. Rev.*, *122*, 2573-2586.

Hodges, K. I., Hoskins, B. J., Boyle, J., & Thorncroft, C. (2003). A comparison of recent reanalysis datasets using objective feature tracking: storm tracks and tropical easterly waves. *Mon. Wea. Rev.*, *131*, 2012-2037.

Hodges, K. I., Hoskins, B. J., Boyle, J., & Thorncroft, C. (2004). Corrigendum. *Mon. Wea. Rev.*, *132*, 1325-1327.

Hodges, K. I., Lee, R. W., & Bengtsson, L. (2011). A comparison of extratropical cyclones in recent reanalyses ERA-Interim, NASA MERRA, NCEP CFSR, and JRA-25. *J. Climate*, *24*, 4888-4906.

Hoskins, B. J., & Hodges, K. I. (2002). New perspectives on the Northern Hemisphere winter storm tracks. *J. Atmos. Sci.*, *59*, 1041-1061.

Hurrell, J. W. (1995). Decadal trends in the North Atlantic Oscillation: regional temperature and precipitation. *Science*, *269*, 676-679.

Hurrell, J. W., & Deser, C. (2009). North Atlantic climate variability: the role of the North Atlantic Oscillation. *J. Marine Sys.*, *78*, 28-41.

Hurrell, J. W., & van Loon, H. (1997). Decadal variations in climate associated with the North Atlantic Oscillation. *Clim. Change*, *36*, 301-326.

Jahnke-Bornemann, A., & Brümmer, B. (2009). The Iceland–Lofotes pressure difference: different states of the North Atlantic low-pressure zone. *Tellus*, *61A*, 466-475.

König, W., Sausen, R., & Sielmann, F. (1993). Objective identification of cyclones in GCM simulations. *J. Climate*, *6*, 2217-2231.

Murray, R. J., & Simmonds, I. (1991). A numerical scheme for tracking cyclone centres from digital data. Part I: Development and operation of the scheme. *Aust. Meteorol. Mag.*, *39*, 155-166.

Nawri, N. (2013). *Large-scale atmospheric conditions associated with major avalanche cycles and cold season weather hazards over Iceland* (Report VÍ 2013-004). Reykjavik, Iceland: Icelandic Meteorological Office.

Raible, C. C., Della-Marta, P. M., Schwierz, C., Wernli, H., & Blender, R. (2008). Northern Hemisphere extratropical cyclones: A comparison of detection and tracking methods and different reanalyses. *Mon. Wea. Rev.*, *136*, 880-897.

Rogers, J. C. (1997). North Atlantic storm track variability and its association to the North Atlantic Oscillation and climate variability of northern Europe. *J. Climate*, *10*, 1636-1647.

Rudeva, I., & Gulev, S. K. (2007). Climatology of cyclone size characteristics and their changes during the cyclone life cycle. *Mon. Wea. Rev.*, *135*, 2568-2587.

Rudeva, I., & Gulev, S. K. (2011). Composite analysis of North Atlantic extratropical cyclones in NCEP–NCAR reanalysis data. *Mon. Wea. Rev.*, *139*, 1419-1446.

Schneidereit, A., Blender, R., Fraedrich, K., & Lunkeit, F. (2007). Icelandic climate and North Atlantic cyclones in ERA-40 reanalyses. *Meteorol. Z.*, *16*(1), 17-23.

Serreze, M. C. (1995). Climatological aspects of cyclone development and decay in the Arctic. *Atmos.-Oce.*, *33*(1), 1-23.

Serreze, M. C., Box, J. E., Barry, R. G., & Walsh, J. E. (1993). Characteristics of Arctic synoptic activity, 1952 – 1989. *Meteorol. Atmos. Phys.*, *51*, 147-164.

Serreze, M. C., Carse, F., Barry, R. G., & Rogers, J. C. (1997). Icelandic Low cyclone activity: Climatological features, linkages with the NAO, and relationships with recent changes in the Northern Hemisphere circulation. *J. Climate*, *10*, 453-464.

Sickmöller, M., Blender, R., & Fraedrich, K. (2000). Observed winter cyclone tracks in the Northern Hemisphere in re-analysed ECMWF data. *Q. J. R. Meteorol. Soc.*, *126*, 591-620.

Simmons, A., Uppala, S., Dee, D., & Kobayashi, S. (2006). ERA-Interim: New ECMWF reanalysis products from 1989 onwards. *ECMWF Newsletter*, *110*, 25-35.

Sinclair, M. R. (1997). Objective identification of cyclones and their circulation intensity, and climatology. *Wea. Forecast.*, *12*, 595-612.

Skeie, P. (2000). Meridional flow variability over the Nordic seas in the Arctic Oscillation framework. *Geophys. Res. Lett.*, *27*(16), 2569-2572.

Trigo, I. F. (2006). Climatology and interannual variability of storm-tracks in the Euro-Atlantic sector: A comparison between ERA- 40 and NCEP/NCAR reanalyses. *Climate Dyn.*, *26*, 127-143.

Trigo, R. M., Valente, M. A., Trigo, I. F., Miranda, P. M. A., Ramos, A. M., Paredes, D., & García-Herrera, R. (2008). The impact of the North Atlantic wind and cyclone trends on European precipitation and significant wave height in the Atlantic. *Trends Direct. Clim. Res.*, *1146*, 212-234.

Ulbrich, U., Leckebusch, G. C., & Pinto, J. G. (2009). Extra-tropical cyclones in the present and future climate: A review. *Theor. Appl. Climatol.*, *96*, 117-131.

Uppala, S. M., Kållberg, P. W., Simmons, A. J., Andrae, U., da Costa Bechtold, V., Fiorino, M., . . . others (2005). The ERA-40 re-analysis. *Q. J. R. Meteorol. Soc.*, *131*, 2961-3012.

van Loon, H., & Rogers, J. C. (1978). The seesaw in winter temperatures between Greenland and Northern Europe. Part I: General description. *Mon. Wea. Rev.*, *106*, 296-310.

Wang, X. L., Feng, Y., Compo, G. P., Swail, V. R., Zwiers, F. W., Allan, R. J., & Sardeshmukh, P. D. (2013). Trends and low frequency variability of extra-tropical cyclone activity in the ensemble of twentieth century reanalysis. *Clim. Dyn.*, *40*, 2775-2800.

Wang, X. L., Swail, V. R., & Zwiers, F. W. (2006). Climatology and changes of extratropical cyclone activity: comparison of ERA-40 with NCEP-NCAR reanalysis for 1958-2001. *J. Climate*, *19*, 3145-3166.

Wernli, H., & Schwierz, C. (2006). Surface cyclones in the ERA-40 dataset (1958-2001). Part I: Novel identification method and global climatology. *J. Atmos. Sci.*, *63*, 2486-2507.

Wu, B., Wang, J., & Walsh, J. E. (2006). Dipole anomaly in the winter Arctic atmosphere and its association with sea ice motion. *J. Climate*, *19*, 210-225.